

Designing a P2-type cathode material with Li in both Na and transition metal layers for Na-ion batteries

Jianxiang Gao(高健翔), Kai Sun(孙凯), Hao Guo(郭浩), Zhengyao Li(李正耀), Jianlin Wang(王建林), Xiaobai Ma(马小柏), Xuedong Bai(白雪东), and Dongfeng Chen(陈东风)

Citation: Chin. Phys. B, 2022, 31 (**9**): 098201. DOI: 10.1088/1674-1056/ac6b21
Journal homepage: http://cpb.iphy.ac.cn; http://iopscience.iop.org/cpb

What follows is a list of articles you may be interested in

Mg-doped layered oxide cathode for Na-ion batteries

Yuejun Ding(丁月君), Feixiang Ding(丁飞翔), Xiaohui Rong(容晓晖), Yaxiang Lu(陆雅翔), and Yong-Sheng Hu(胡勇胜)

Chin. Phys. B, 2022, 31 (**6**): 068201. DOI: 10.1088/1674-1056/ac523b

Analysis on diffusion-induced stress for multi-layer spherical core-shell electrodes in Li-ion batteries

Siyuan Yang(杨思源), Chuanwei Li(李传崴), Zhifeng Qi(齐志凤), Lipan Xin(辛立攀), Linan Li(李林安), Shibin Wang(王世斌), and Zhiyong Wang(王志勇)

Chin. Phys. B, 2021, 30 (**9**): 098201. DOI: 10.1088/1674-1056/ac11de

In situ formed FeS_2@CoS cathode for long cycling life lithium-ion battery

Xin Wang(王鑫), Bojun Wang(汪博筠), Jiachao Yang(杨家超), Qiwen Ran(冉淇文), Jian Zou(邹剑), Pengyu Chen(陈鹏宇), Li Li(李莉), Liping Wang(王丽平), and Xiaobin Niu(牛晓滨)

Chin. Phys. B, 2021, 30 (**8**): 088201. DOI: 10.1088/1674-1056/abe9ab

Failure analysis with a focus on thermal aspect towards developing safer Na-ion batteries

Yuqi Li(李钰琦), Yaxiang Lu(陆雅翔), Liquan Chen(陈立泉), Yong-Sheng Hu(胡勇胜)

Chin. Phys. B, 2020, 29 (**4**): 048201. DOI: 10.1088/1674-1056/ab7906

Hard carbons derived from pine nut shells as anode materials for Na-ion batteries

Hao Guo(郭浩), Kai Sun(孙凯), Yaxiang Lu(陆雅翔), Hongliang Wang(王洪亮), Xiaobai Ma(马小柏), Zhengyao Li(李正耀), Yong-Sheng Hu(胡勇胜), Dongfeng Chen(陈东风)

Chin. Phys. B, 2019, 28 (**6**): 068203. DOI: 10.1088/1674-1056/28/6/068203

RAPID COMMUNICATION

Designing a P2-type cathode material with Li in both Na and transition metal layers for Na-ion batteries

Jianxiang Gao(高健翔)[1], Kai Sun(孙凯)[1,†], Hao Guo(郭浩)[1], Zhengyao Li(李正耀)[1], Jianlin Wang(王建林)[2], Xiaobai Ma(马小柏)[1], Xuedong Bai(白雪东)[2], and Dongfeng Chen(陈东风)[1,‡]

[1] *China Institute of Atomic Energy, Beijing* 102413, *China*

[2] *State Key Laboratory for Surface Physics, Institute of Physics, Chinese Academy of Sciences, Beijing* 100190, *China*

(Received 13 January 2022; revised manuscript received 22 April 2022; accepted manuscript online 28 April 2022)

P2-type layered oxides have been considered as promising cathode materials for Na-ion batteries, but the capacity decay resulting from the Na^+/vacancy ordering and phase transformation limits their future large-scale applications. Herein, the impact of Li-doping in different layers on the structure and electrochemical performance of P2-type $Na_{0.7}Ni_{0.35}Mn_{0.65}O_2$ is investigated. It can be found that Li ions successfully enter both the Na and transition metal layers. The strategy of Li-doping can improve the cycling stability and rate capability of P2-type layered oxides, which promotes the development of high-performance Na-ion batteries.

Keywords: $Na_{0.7}Ni_{0.35}Mn_{0.65}O_2$, Li-doping, P2-type cathode, Na-ion batteries

PACS: 82.45.Fk, 88.80.ff, 71.20.Dg **DOI:** 10.1088/1674-1056/ac6b21

1. Introduction

The rapid development and widespread applications of Li-ion batteries (LIBs) have caused the increasing demand and cost of lithium resources. Na-ion batteries (NIBs), due to the high abundance and uniform distribution of Na sources, are considered as an appealing alternative to Li-ion batteries (LIBs), especially on applications of large-scale energy storage.[1–3] The cathode materials with various structures, including layered transition metal oxides,[4–9] Na super ionic conductors (NASICON),[10,11] prussian blue analogues,[12–15] and organic compounds,[16] etc., have been synthesized and investigated. Among these materials, layered transition-metal oxides (Na_xTMO_2, TM = transition metal) are one of the most promising candidates for commercial application due to their feasible preparation process and high theoretical capacity.[17,18] According to the coordination environments of Na and stacking modes of oxygen, Na_xTMO_2 have been mainly classified into P2 and O3 types, proposed by Delmas.[19] "P" and "O" represent that Na^+ ions are coordinated in prismatic and octahedral environments, respectively, while the number "2" or "3" refers to the repeated layers in an unit cell. Compared with the O3-type structure, Na ions can migrate between neighboring prismatic sites directly in the P2-type structure, which results in a lower diffusion barrier and therefore enhanced rate performance.[20,21]

However, the P2-type structures suffer from the complicated phase transition and Na^+/vacancy ordering, leading to step-like voltage curves, capacity decay, and poor cycling life.[22,23] For example, although P2-$Na_{2/3}Ni_{1/3}Mn_{2/3}O_2$ delivers a high-operation voltage and high capacity, it still has problems such as the severe capacity fading by the P2-O2 phase transition when charging to above 4.0 V.[24,25] To improve the cycling stability, element doping (Cu, Ti, Mg, F, etc.),[26–30] and surface coating[31] have been proven to be effective strategies. Previous reports show that Li-doping can stabilize the structure by suppressing the Jahn–Teller effect of Mn^{3+} and delaying the detrimental phase transitions.[32,33] Considering that the ionic radius of Li^+ (0.76 Å) is similar to that of Ni^{2+} (0.69 Å), the Li-ions doped in layered Na_xTMO_2 tends to occupy the TM layers.[34,35] In addition, with increasing the amount of Li, extra diffraction peaks at $\sim 18°$ and $\sim 41°$ appear, which can be assigned to the monoclinic Li_2MnO_3 component ($C2/m$) or the rhombohedral O3-type structure ($R\bar{3}m$).[36,37]

In this work, we have successfully synthesized the phase-pure samples of Li-free $Na_{0.7}Ni_{0.35}Mn_{0.65}O_2$ (Li0), $Na_{0.75}[Li_{0.05}Ni_{0.3}Mn_{0.65}]O_2$ with Li-doping in the TM layers (Li5), and $Na_{0.7}Li_{0.05}[Li_{0.05}Ni_{0.3}Mn_{0.65}]O_2$ with Li-doping in both the Na and TM layers simultaneously (Li10). The x-ray diffraction results show that Li ions locate at the TM layers in the Li5 sample and both the TM layers and Na layers in the Li10 sample. The electrochemical performance results demonstrate that the rate and cycle performance are improved after Li doping. In the voltage range of 2.0–4.0 V, the capacity of Li-free Li0 electrode is only ~ 39 mAh/g at 10 C, while the Li-doped Li5 and Li10 electrodes can display the capacities of about 65 and 64 mAh/g at 10 C, respectively. The Li0, Li5, and Li10 electrodes deliver the capacity retentions of 76.5%,

†Corresponding author. E-mail: ksun@ciae.ac.cn
‡Corresponding author. E-mail: dongfeng@ciae.ac.cn

© 2022 Chinese Physical Society and IOP Publishing Ltd

81.7%, and 88.5% after 300 cycles in the voltage range of 2.0–4.0 V, respectively, indicating the enhanced cycling stability after Li-doping.

2. Experiment

2.1. Material synthesis

$Na_{0.7}Ni_{0.35}Mn_{0.65}O_2$ (Li0), $Na_{0.75}[Li_{0.05}Ni_{0.3}Mn_{0.65}]O_2$ (Li5), and $Na_{0.7}Li_{0.05}[Li_{0.05}Ni_{0.3}Mn_{0.65}]O_2$ (Li10) samples were synthesized by a solid-state method using Na_2CO_3(99%), Li_2CO_3(99%), NiO(99%), and MnO_2(98%) as precursors. The raw materials were mixed and ground in an agate mortar for 25 min and pressed into a pellet under a pressure of 12 MPa. Then these pellets were fired at 950 °C for 15 h in muffle furnace under air and cooled to room temperature naturally.

2.2. Structure characterization

X-ray diffraction (XRD) patterns were collected on an x-ray diffractometer (D8 Bruker) using Cu K_α radiation by measuring the diffraction angle (2θ) range of 10°–70°. The refinements of XRD data were performed with FullProf software using the Rietveld method.[38] The morphology and microstructure were investigated by a scanning electron microscope (SEM, Gemini 300) and a high-resolution transmission electron microscope (HRTEM, FEI Tecnai F20).

2.3. Electrochemical measurement

These working electrodes were prepared by spreading the slurry of the active materials, acetylene black and the polyvinylidene fluoride (PVDF) binder with a weight ratio of 8:1:1 on Al foil. Then these electrodes were dried at 120 °C under vacuum for 10 h. The coin-type cells (CR2032) were assembled with Na foil as the counter electrode, 1.0 M $NaClO_4$/propylene carbonate (PC) with 5% fluoroethylene carbonate (FEC) in volume as electrolyte and a glass fiber (GF/D) as the separator in an argon-filled glove box. The electrochemical testing on different voltage ranges was carried out using a Neware CT-4000 battery test system.

3. Results and discussion

The crystal structures of the $Na_{0.7}Li_{0.05}[Li_{0.05}Ni_{0.3}Mn_{0.65}]O_2$ (Li10), $Na_{0.75}[Li_{0.05}Ni_{0.3}Mn_{0.65}]O_2$ (Li5), and $Na_{0.7}Ni_{0.35}Mn_{0.65}O_2$ (Li0) were initially characterized using x-ray diffraction (XRD). As shown in Fig. 1(a), all the samples can be indexed to the P2-type structure (space group of $P6_3/mmc$) without any second phase. The influence of higher Li content on the crystal structure was also investigated. The $Na_{0.66}Li_{0.09}[Li_{0.05}Ni_{0.3}Mn_{0.65}]O_2$ and $Na_{0.68}Li_{0.07}[Li_{0.05}Ni_{0.3}Mn_{0.65}]O_2$ samples with higher Li content show the extra weak diffraction peak at around 18° in Fig. S1, which can be assigned to the monoclinic Li_2MnO_3 component ($C2/m$), consistent with the previous reports.[36,37] Therefore, the three pure P2-phase samples of Li0, Li5 and Li10 are mainly studied in this work. The XRD patterns of the Li0, Li5 and Li10 are further refined based on the Rietveld method. It can be seen in Figs. 1(b)–1(d) that the refinement results are well in agreement with the observed data.

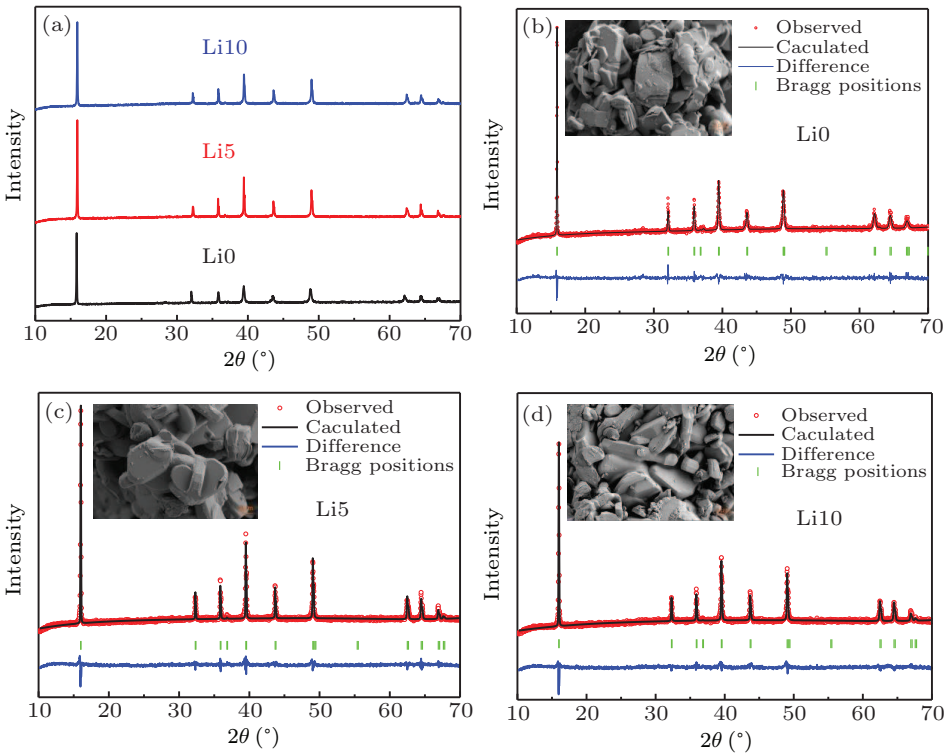


Fig. 1. (a) XRD patterns of the Li10, Li5, and Li10 samples. Refined XRD patterns and the SEM images of (b) Li0, (c) Li5, and (d) Li0.

The corresponding lattice parameters, atomic occupancies and isotropic displacement parameters are presented in Tables S1–S3. Figure 2 exhibits the reconstructed crystal structure of the Li0, Li5, and Li10 samples according to the XRD refinements. For all the samples, Ni^{2+} ions and Mn^{4+} ions locate at the 2*a* (0,0,0) site, while the Na ions locate at the two prismatic sites in the Na layer (2*b* (0, 0, 0.25) site and 2*d* (0.6667, 0.3333, 0.25) site). The Li ions locate at 2*a* sites in the TM layers in the Li5 material host, while the Li ions locate at both the TM layers and Na layers simultaneously in the Li10 material host.

As shown in Table 1, Li doping has little impact on the lattice parameter *a*, which is consistent with the previous report.[39] This may be related to the similar sizes of Li^{+} (0.76 Å) and Ni^{2+} (0.69 Å), because the lattice parameter *a* represents the atomic distance in the *ab* plane. On the contrary, the lattice parameter *c* reduces significantly after Li doping. The reduced Na shielding effect by a higher Na/Li content in Li5 and Li10 compared with Li0 can account for the reduction in lattice parameter *c*.[40]

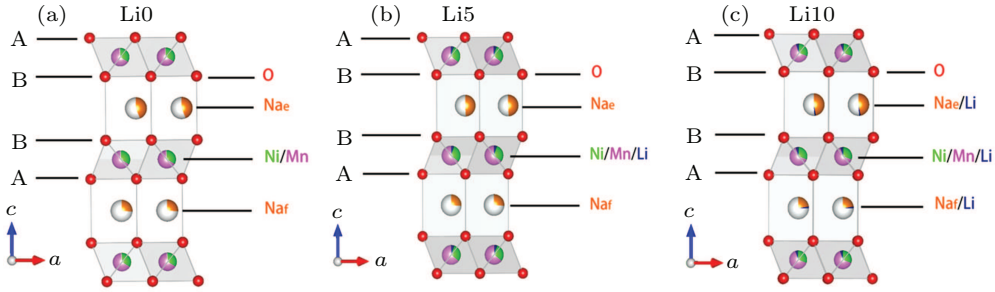


Fig. 2. Reconstructed crystal structures of (a) Li0, (b) Li5, and (c) Li10 materials.

Table 1. Lattice parameters obtained by using Rietveld refinements.

Sample		Li0	Li5	Li10
Lattice parameters	*a* (Å)	2.8871(6)	2.8882(8)	2.8867(3)
	b (Å)	2.8871(6)	2.8882(8)	2.8867(3)
	c (Å)	11.1520(3)	11.0735(4)	11.0803(5)
	volume (Å^3)	80.5031(2)	79.9987(3)	79.9620(4)

The morphologies of Li0, Li5, and Li10 samples were investigated by scanning electron microscopy (SEM). As presented in Figs. 1(b)–1(d), the as-prepared samples are composed of blocky-shaped particles and the distribution of particle size is in the range of 2–6 μm. The high-resolution transmission electron microscopy (HRTEM) image of the Li10 sample in Fig. 3(a) reveals that the interplanar spacing of lattice fringes is ∼ 0.250 nm, which matches well with the (100) plane of the P2-type structure. Selected-area electron diffraction (SAED) was applied to obtain the specific structural information of Li10 in Fig. 3(b). The bright spots can be indexed to the representative reflections of the P2-type structure viewed along the [001] axis. Figures 3(c)–3(g) show the energy-dispersive spectroscopy (EDS) mapping of Li10, which indicate that Na, Ni, Mn and O elements are uniformly distributed in the Li10 material.

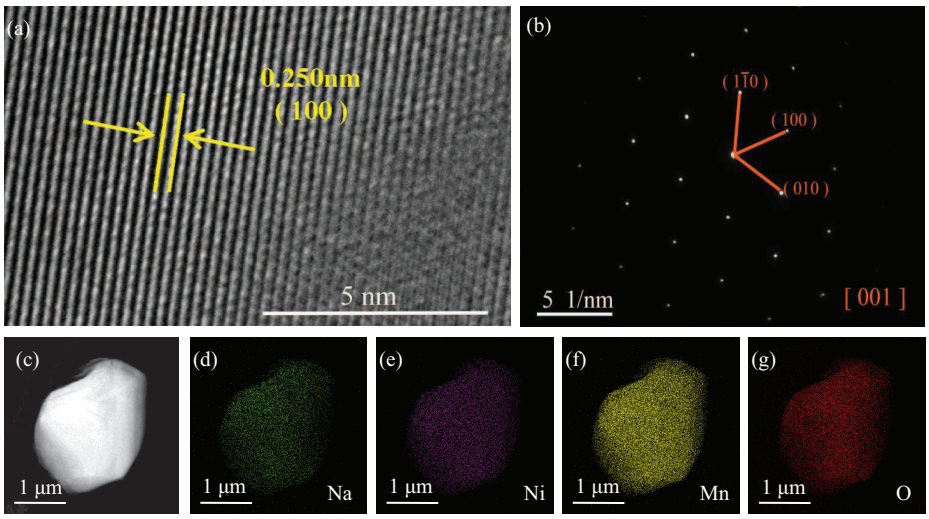


Fig. 3. Characterization of the as-prepared Li10 material. (a) HRTEM image, (b) SAED pattern, and (c)–(g) TEM-EDS mapping results for the selected elements.

The electrochemical performances of Li0, Li5, and Li10 electrodes were investigated by galvanostatic charge/discharge tests. Figures 4(a)–4(c) show the first three charge–discharge profiles of these electrodes in the voltage range of 1.5–4.2 V versus Na^+/Na at a rate of 0.1 C. The Li0 electrode shows several voltage plateaus, which are closely related to the P2–O2 phase transition and Na^+/vacancy ordering.[22,25] It can be observed that Li5 and Li10 electrodes exhibit the smoother charge/discharge curves, indicating the suppressed phase transition and Na^+/vacancy ordering, similar to the reported $Na_{1.0}Li_{0.2}Ni_{0.25}Mn_{0.7}O_2$[41] and $Na_{0.8}[Li_{0.12}Ni_{0.22}Mn_{0.66}]O_2$.[33] Figure 4(d) shows the cycle performances of Li0, Li5 and Li10 electrodes at 0.5 C in the voltage range of 1.5–4.2 V. The results demonstrate that Li doping can improve the capacity retention from 46.9% of Li0 to 70.0% of Li5 and 80.7% of Li10. The improvement of capacity retention can be attributed to the stabilized structure by Li doping.[32,42]

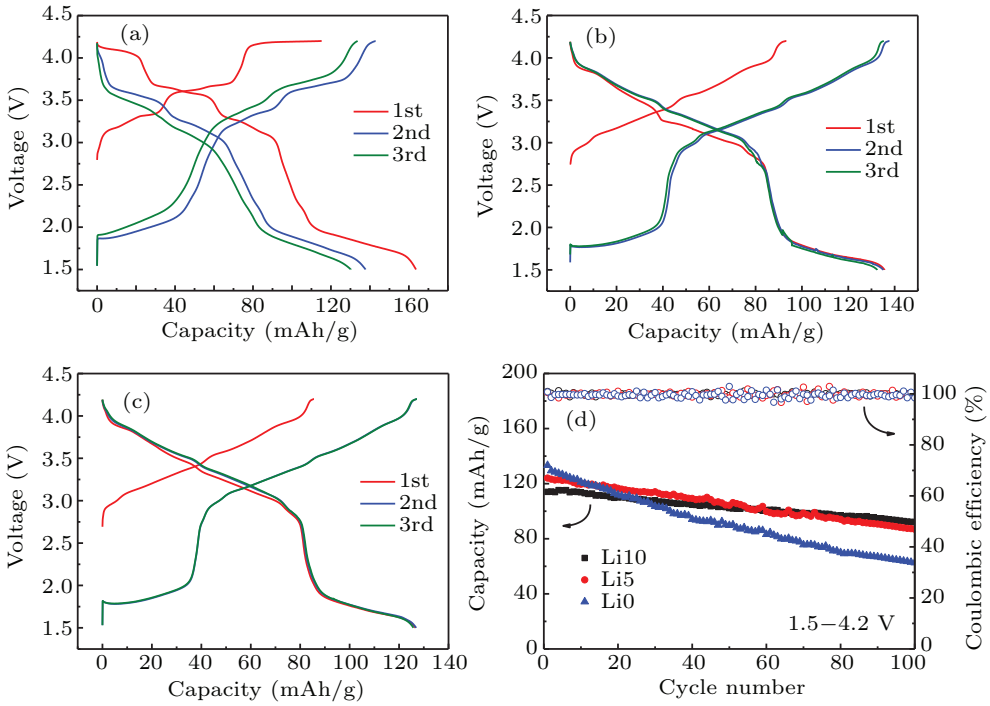


Fig. 4. Charge-discharge profiles of (a) Li0, (b) Li5, and (c) Li10 at 0.1 C in the voltage range of 1.5–4.2 V vs. Na^+/Na. (d) Cycle performances of the Li0, Li5, and Li10 electrodes at 0.5 C after 100 cycles in the voltage range of 1.5–4.2 V.

To investigate the influence of Li-doping in different voltage ranges, the cycle performance was studied in the voltage ranges of 1.5–4.0 V, 2.0–4.2 V, and 2.0–4.0 V, and the results are shown in Fig. S2 in the supporting information. The capacity retention of Li0, Li5, and Li10 electrodes in various voltage ranges are presented in Table 2. It can be found that the cycle performances in different voltage ranges are improved after Li doping. For example, the capacity retention of Li0 is 91.4% in the voltage range of 2.0–4.0 V, which increases to 95.2% of Li5 and 97.1% of Li10, respectively. Previous reports have proved that the Mn^{4+}/Mn^{3+} redox causes the structure instability due to the Jahn–Teller effect of Mn^{3+} when the voltage is lower than 2.0 V.[22,24] On the other hand, the P2-type cathodes always undergo the detrimental P2-O2 phase transformation with a large volume change upon charging to over 4.0 V, causing the severe capacity fading.[25,43] The study indicates that the electrodes exhibit the best cycle performance in the voltage range of 2.0–4.0 V.[42,44]

Figure 5(a) exhibits the long-term cycle performances of Li0, Li5, and Li10 electrodes at 0.5 C in the voltage range of 2.0–4.0 V. The capacity retentions of Li0, Li5, and Li10 electrodes after 300 cycles are 76.5%, 81.7%, and 88.5%. The Li10 electrode with Li doping in both the Na and TM layers simultaneously exhibits the best cycling stability. Figure 5(b) further compares the rate performances of these electrodes at different current densities in the voltage range of 2.0–4.0 V. The capacities of Li0 electrode are 93, 89, 81, 60, and 39 mAh/g at the rates of 0.1, 0.5, 2, 5, and 10 C, respectively. Interestingly, the Li10 electrode delivers the capacities of 92, 89, 84, 75, and 64 mAh/g, respectively, which are almost equal to those of Li5 electrode. These results demonstrate that Li doping can improve cycling stability and rate performance.

Table 2. The capacity retention of Li0, Li5, and Li10 electrodes at 0.5 C after 100 cycles in different voltage ranges.

Voltage	Li0	Li5	Li10
1.5–4.2 V	46.9%	70.0%	80.7%
1.5–4.0 V	49.4%	71.3%	81.5%
2.0–4.2 V	80.1%	89.2%	93.7%
2.0–4.0 V	91.4%	95.2%	97.1%

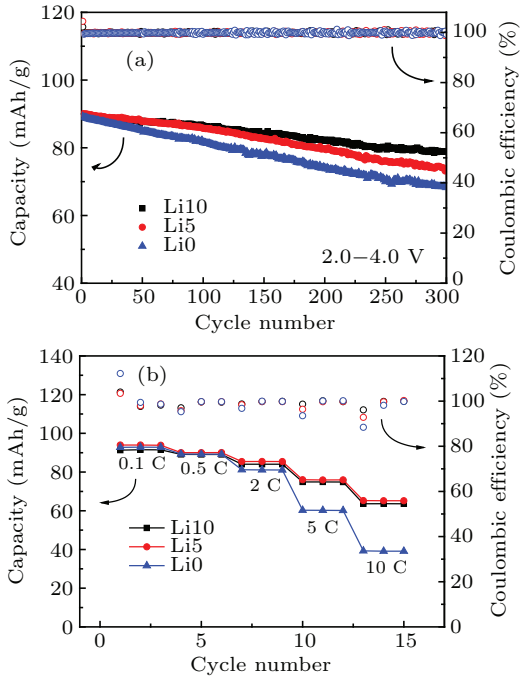


Fig. 5. (a) Cycle performances of the Li10, Li5, and Li0 electrodes at 0.5 C after 300 cycles in the voltage range of 2.0–4.0 V. (b) Rate performances of the Li0, Li5, and Li10 electrodes in the voltage range of 2.0–4.0 V at various rates.

To investigate the influence of Li doping on structure evolution during the charge and discharge process, the *ex situ* XRD patterns of Li10 electrode at different voltages are collected. As demonstrated in Fig. 6, the (002) diffraction peak of Li10 electrode shifts continually to lower angle upon charging, corresponding to the expansion of the interlayer distance. In the subsequent discharging course, the (002) diffraction peak when discharged to 1.5 V shifts to an angle higher than pristine state due to extra sodium intercalated into electrode. It is noteworthy that there is not any new peaks appearing in the whole charging and discharging course, indicating that the P2-type structure is maintained well without the common P2–O2 phase transition.[25] This solid-solution reaction contributes to the excellent cycle retention and good rate performance. HRTEM is also used to analyze the microstructure changes after cycling. As shown in Fig. S3(a) in the supporting information, it can be observed that the HRTEM image of Li0 electrode charged at 4.2 V shows the dislocation. This phenomenon is absent in the HRTEM image of the Li-doped Li10 electrode in Fig. S3(b), which is helpful for improving cycling stability. These *ex situ* XRD and HRTEM results prove that Li doping can suppress the P2-O2 phase transition and enhance structure stability, thus improving cycling stability.

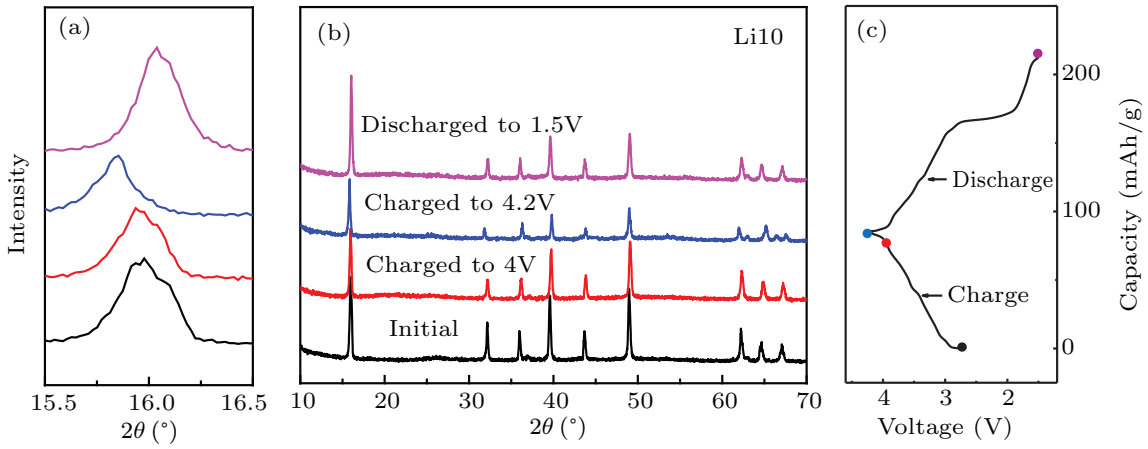


Fig. 6. *Ex situ* XRD patterns of Li10 at different charge/discharge states: (a) the enlargement parts of the (002) peak, (b) the whole patterns between 10° and 70°, (c) the corresponding charge/discharge profiles during the *ex situ* XRD tests.

4. Conclusion

In summary, a series of Li0, Li5, and Li10 cathode materials are synthesized by a solid-state method. The XRD results show that Li ions can incorporate in both the Na and transition metal layers. Electrochemical measurement results demonstrate that Li doping can largely improve the cycle and rate performance. The Li-doped Li5 andLi10 electrodes deliver 65 and 64 mAh/g at the high rate of 10 C, while Li-free Li0 electrode only delivers 39 mAh/g at 10 C in the voltage range of 2.0–4.0 V. The Li10 electrode exhibits the excellent cycling stability in the voltage range of 2.0–4.0 V with the capacity retention of 88.5% after 300 cycles, higher than those of Li0 and Li5 electrodes. *Ex situ* XRD and HRTEM results show that P2-phase maintains well after Li doping, thus enabling improved electrochemical performances. It can be concluded that incorporating Li into both the Na and transition metal layers of P2-type cathodes is a useful strategy for designing high-performance cathode materials in Na-ion batteries.

Acknowledgements

Project supported by the National Natural Science Foundation of China (Grant Nos. 12105372 and 51991344), President's Foundation of China Institute of Atomic Energy (Grant No. 16YZ202212000201), and Chinese Academy of Sciences (Grant No. XDB33000000).

References

[1] Gao R M, Zheng Z J, Wang P F, Wang C Y, Ye H and Cao F F 2020 *Energy Storage Mater.* **30** 9

[2] Li Y, Lu Y, Zhao C, Hu Y S, Titirici M M, Li H, Huang X and Chen L 2017 *Energy Storage Mater.* **7** 130

[3] Yu J Z, Hu Y S, Li H, Huang X J and Chen L Q 2017 *Acta Phys. Sin.* **66** 088201 (in Chinese)

[4] Wei F, Zhang Q, Zhang P, Tian W, Dai K, Zhang L, Mao J and Shao G 2021 *J. Electrochem. Soc.* **168** 050524

[5] Guo G C, Wang C, Ming B M, Luo S W, Su H, Wang B Y, Zhang M, Yu H J and Wang R Z 2018 *Chin. Phys. B* **27** 118801

[6] Mu L Q, Hu Y S and Chen L Q 2015 *Chin. Phys. B* **24** 038202

[7] Guo H, Avdeev M, Sun K, Ma X, Wang H, Hu Y and Chen D 2021 *Chem. Eng. J.* **412** 128704

[8] Li Z Y, Gao R, Sun L, Hu Z and Liu X 2017 *Electrochim. Acta* **223** 92

[9] Xu S Y, Wu X Y, Li Y M, Hu Y S and Chen L Q 2014 *Chin. Phys. B* **23** 118202

[10] Lavela P, Klee R and Tirado J L 2021 *Sustain. Energy Fuels* **5** 4095

[11] Wang J, Wang Y, Seo D H, Shi T, Chen S, Tian Y, Kim H and Ceder G 2020 *Adv. Energy Mater.* **10** 1903968

[12] Wang L, Lu Y, Liu J, Xu M, Cheng J, Zhang D and Goodenough J B 2013 *Angew. Chem. Int. Edit.* **52** 1964

[13] Wang L, Song J, Qiao R, Wray L A, Hossain M A, Chuang Y D, Yang W, Lu Y, Evans D, Lee J J, Vail S, Zhao X, Nishijima M, Kakimoto S and Goodenough J B 2015 *J. Am. Chem. Soc.* **137** 2548

[14] Ren W, Qin M, Zhu Z, Yan M, Li Q, Zhang L, Liu D and Mai L 2017 *Nano Lett.* **17** 4713

[15] Lu Y, Wang L, Cheng J and Goodenough J B 2012 *Chem. Commun.* **48** 6544

[16] Luo W, Allen M, Raju V and Ji X 2014 *Adv. Energy Mater.* **4** 1400554

[17] Han M H, Gonzalo E, Singh G and Rojo T 2015 *Energy Environ. Sci.* **8** 81

[18] Kubota K, Kumakura S, Yoda Y, Kuroki K and Komaba S 2018 *Adv. Energy Mater.* **8** 1703415

[19] Delmas C, Fouassier C and Hagenmuller P 1980 *Physica B+C* **99** 81

[20] Yabuuchi N, Kubota K, Dahbi M and Komaba S 2014 *Chem. Rev.* **114** 11636

[21] Pan H, Hu Y S and Chen L 2013 *Energy Environ. Sci.* **6** 2338

[22] Zhang J, Wang W, Wang W, Wang S and Li B 2019 *ACS Appl. Mater. Interfaces* **11** 22051

[23] Jung Y H, Christiansen A S, Johnsen R E, Norby P and Kim D K 2015 *Adv. Funct. Mater.* **25** 3227

[24] Wen Y, Wang B, Zeng G, Nogita K, Ye D and Wang L 2015 *Chem. Asian J.* **10** 661

[25] Lu Z and Dahn J R 2001 *J. Electrochem. Soc.* **148** A1225

[26] Wang J, Liu H, Yang Q, Hu B, Geng F, Zhao C, Lin Y and Hu B 2020 *ACS Appl. Mater. Interfaces* **12** 34848

[27] Li Z, Kong W, Yu Y, Yang W, Yang J and Liu X 2021 *J. Phys. Chem. C* **125** 8105

[28] Tang K, Huang Y, Xie X, Cao S, Liu L, Liu H, Luo Z, Wang Y, Chang B, Shu H and Wang X 2020 *Chem. Eng. J.* **399** 125725

[29] Li Z Y, Ma X, Guo H, He L, Li Y, Wei G, Sun K and Chen D 2021 *ACS Appl. Energy Mater.* **4** 5687

[30] Liu K, Tan S, Moon J, Jafta C J, Li C, Kobayashi T, Lyu H, Bridges C A, Men S, Guo W, Sun Y, Zhang J, Paranthaman M P, Sun X G and Dai S 2020 *Adv. Energy Mater.* **10** 2070087

[31] Jo J H, Choi J U, Konarov A, Yashiro H, Yuan S, Shi L, Sun Y K and Myung S T 2018 *Adv. Funct. Mater.* **28** 1705968

[32] Yang L, Li X, Liu J, Xiong S, Ma X, Liu P, Bai J, Xu W, Tang Y, Hu Y Y, Liu M and Chen H 2019 *J. Am. Chem. Soc.* **141** 6680

[33] Xu J, Lee D H, Clement R J, Yu X, Leskes M, Pell A J, Pintacuda G, Yang X Q, Grey C P and Meng Y S 2014 *Chem. Mater.* **26** 1260

[34] Jin T, Wang P F, Wang Q C, Zhu K, Deng T, Zhang J, Zhang W, Yang X Q, Jiao L and Wang C 2020 *Angew. Chem. Int. Ed.* **59** 14511

[35] Zhao C, Yao Z, Wang Q, Li H, Wang J, Liu M, Ganapathy S, Lu Y, Cabana J, Li B, Bai X, Aspuru-Guzik A, Wagemaker M, Chen L and Hu Y S 2020 *J. Am. Chem. Soc.* **142** 5742

[36] Wang Y, Hu G, Peng Z, Cao Y, Lai X, Qi X, Gan Z, Li W, Luo Z and Du K 2018 *J. Power Sources* **396** 639

[37] Ding Z, Liu Y, Tang Q, Jiang Q, Lu J, Xiao Z, Yao P, Monasterio M, Wu J and Liu X 2018 *Electrochim. Acta* **292** 871

[38] Rodríguez-Carvajal J 1993 *Physica B* **192** 55

[39] Xie Y, Gabriel E, Fan L, Hwang I, Li X, Zhu H, Ren Y, Sun C, Pipkin J, Dustin M, Li M, Chen Z, Lee E and Xiong H 2021 *Chem. Mater.* **33** 4445

[40] Zhao C, Wang Q, Yao Z, Wang J, Sánchez-Lengeling B, Ding F, Qi X, Lu Y, Bai X, Li B, Li H, Aspuru-Guzik A, Huang X, Delmas C, Wagemaker M, Chen L and Hu Y S 2020 *Science* **370** 708

[41] Kim D, Kang S H, Slater M, Rood S, Vaughey J T, Karan N, Balasubramanian M and Johnson C S 2011 *Adv. Energy Mater.* **1** 333

[42] Zheng X, Li P, Zhu H, Rui K, Zhao G, Shu J, Xu X, Sun W and Dou S X 2018 *Energy Storage Mater.* **15** 257

[43] Lee D H, Xu J and Meng Y S 2013 *Phys. Chem. Chem. Phys.* **15** 3304

[44] Wang H, Yang B, Liao X Z, Xu J, Yang D, He Y S and Ma Z F 2013 *Electrochim. Acta* **113** 200